Available online at www.sciencedirect.com
ScienceDirect
Surface & Coatings Technology 202 (2008) 3157–3163
SURFACE & COATINGS TECHNOLOGY
www.elsevier.com/locate/surfcoat

Effects of the restructuring of Fe catalyst films on chemical vapor deposition of carbon nanotubes

Huaping Liu [a,b,*], Guo-An Cheng [a,*], Ruiting Zheng [a], Yong Zhao [a,c], Changlin Liang [a]

[a] Key Laboratory of Radiation Beam Technology and Material Modification of Education Ministry, Department of Materials Science and Engineering, Institute of Low Energy Nuclear Physics, Beijing Normal University, Beijing Radiation Center, Beijing 100875, PR China
[b] Department of Physics, Tokyo University of Science, Shinjuku, Tokyo 162-8601, Japan
[c] Department of Physics, Nanchang University, Nanchang 330047, PR China

Received 27 June 2007; accepted in revised form 20 November 2007
Available online 28 November 2007

Abstract

We investigated the restructuring of Fe catalyst films during high temperature processing and its effects on the morphologies of carbon nanotubes (CNTs) arrays synthesized using the thermal chemical vapor deposition (CVD) techniques. Results show that annealing time and gas environment deeply influence the particle size distribution, which determines the morphologies of the corresponding CNT arrays. Fe particles with narrow size distribution were obtained after proper high temperature processing in NH_3, from which higher purity CNT arrays with better-alignment and uniform diameter distribution have been grown.

Keywords: Fe films; Restructuring; Carbon nanotubes; Chemical vapor deposition

1. Introduction

Since their discovery [1], carbon nanotubes (CNTs) attract extensive interests from the scientists in all kinds of fields because of their electrical, chemical and mechanical properties which give them the corresponding potential applications in electronic devices, metallic catalyst supports and enhanced fibers in composites [2–6]. Controlled growth of CNTs is critical for their application, due to the close relationship between their morphologies/nanostructures and their measured properties [4,5]. However, controlled growth of CNTs is still a challenge. To date, the most versatile techniques for synthesizing CNTs have been those based on catalyst-assisted CVD methods. In these CVD methods, catalyst particle size and shape determine the morphologies and nanostructures of CNTs [2]. For this, different methods have been developed to prepare isolated and uniformly distributed metallic catalyst nanoparticles [7–18]. In many cases, metallic catalyst films are used and followed by high temperature processing in H_2, N_2 and NH_3 etc. to form nanoscaled particles [7–9]. Because thin films have a high surface-to-volume ratio, on heating, metallic films may develop holes and may eventually agglomerate into particles with a lower surface-to-volume ratio [19]. With continuously heating, these particles might coalesce due to Ostwald ripening or surface migration [20–22], thus modifying the final distribution of catalyst particles, which determine the morphologies of CNTs obtained [18,23]. This process is strongly dependent on catalyst-substrates interaction [24], the surface morphologies of the pristine metallic films [25], film thickness [26–28], heating time and gas environment [29] etc., which have never been investigated in the view point of the relation between the chemical or physical state of metallic catalysts and the formation state of CNT to control CNT array structures.

In our previous paper [25], we have reported varying deposition angles, which are the angles subtended by the incoming flux and the substrate surface, can well control the surface morphologies of Fe catalyst films. It was found that the

* Corresponding authors. Key Laboratory of Radiation Beam Technology and Material Modification of Education Ministry, Department of Materials Science and Engineering, Institute of Low Energy Nuclear Physics, Beijing Normal University, Beijing Radiation Center, Beijing 100875, PR China. Tel./fax: +86 10 62205403.
E-mail addresses: lhp77616@tom.com (H. Liu), gacheng@bnu.edu.cn (G.-A. Cheng).

0257-8972/$ - see front matter © 2007 Elsevier B.V. All rights reserved.
doi:10.1016/j.surfcoat.2007.11.020

Fe thin films with uniform surface topography could be obtained at 30° of deposition angles. Here, in order to control the formation and distribution of Fe particles, we systematically studied the restructuring of 5 nm of Fe films deposited at 30° of deposition angle during high temperature processing in NH_3 with heating time, and simply discussed the effect of gas environment on the distribution of Fe particles. Further more, we successfully synthesized high-purity and well-aligned CNT arrays with uniform diameters by controlling high temperature processing parameters.

2. Experimental section

N type (111) silicon wafers with a native oxide layer were employed as the substrates of Fe catalyst films. 5 nm of Fe catalyst films were deposited at 30° of deposition angle by employing a metal vapor vacuum arc (MEVVA) system, which has been described in detail in our previous paper [25]. Before deposition, substrates were bombarded to clean the surfaces at 3000 V of negative bias applied on the substrates. The film thickness was monitored in situ by the charge accumulation number measured by the integraph installed on the MEVVA system, and calibrated ex situ by atomic force microscopy. The charge accumulation number is proportional to film thickness.

The thermal treatment of Fe films and subsequent CNT growth were performed in a horizontal furnace with a quartz tube (100 mm in inner diameter and 1500 mm in length) at atmospheric pressure. Typically, the as-deposited Fe catalyst films were loaded into the furnace at room temperature and then heated to 600 °C in H_2. The Fe catalysts were reduced for 60 min at 600 °C and subsequently heated up to the nanotube growth temperature (750 °C) in H_2. When the temperature was stabilized, H_2 was replaced with NH_3 at a flow rate of 200 sccm. Fe catalyst films were annealed for 0–30 min in NH_3. In order to investigate the distribution of nanoscaled Fe particles, we took the catalyst films out for observation at the end of heat treatment in NH_3. The synthesis of CNTs was initialed by introducing the mixture gas of C_2H_2 and H_2 with a flow rate ratio of 100 sccm/

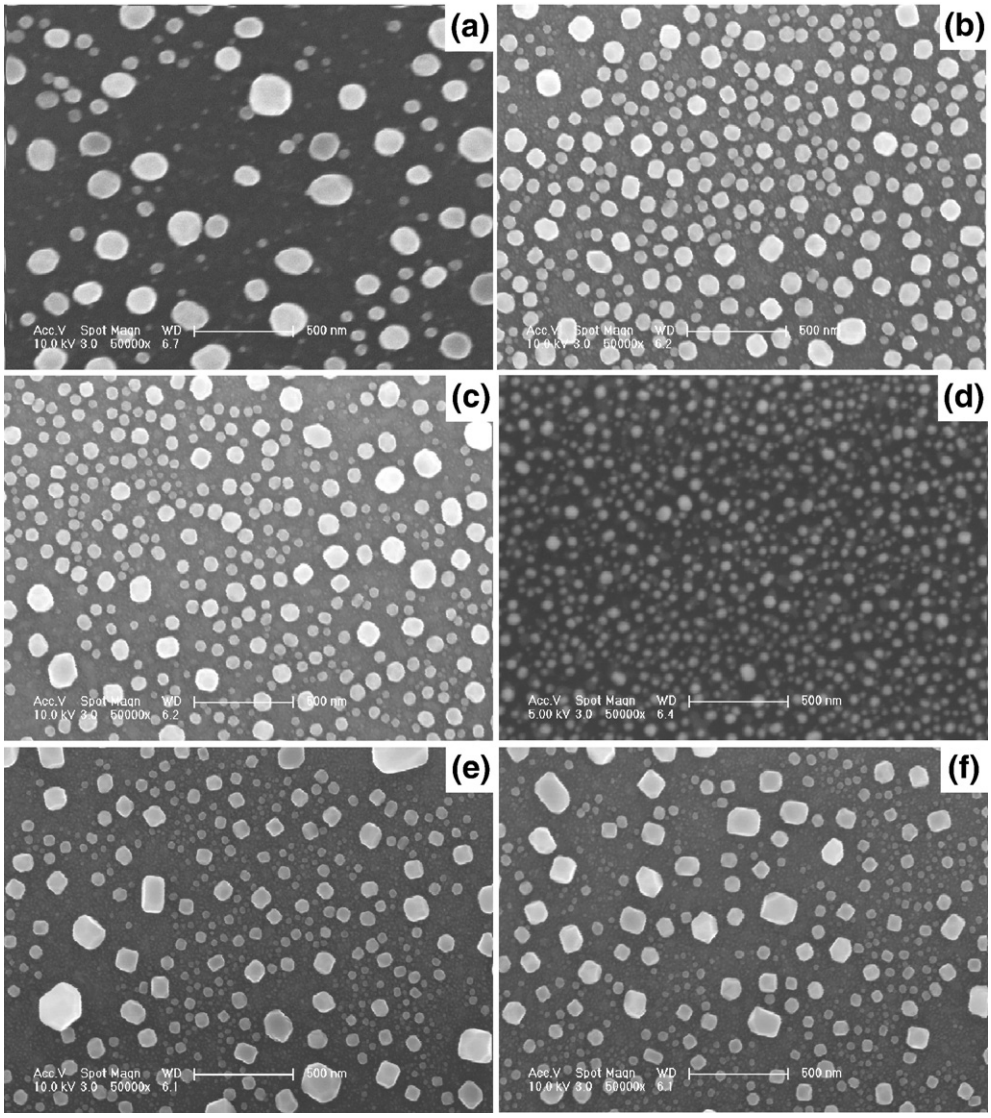

Fig. 1. FESEM images of 5 nm of Fe films after heat treatment in NH_3 for different time. (a) 4 min; (b) 6 min;(c) 8 min; (d) 10 min; (e) 12 min; (f) 14 min.

400 sccm. After growth, the system was cooled down to room temperature in H_2.

Field emission scanning electron microscopy (FESEM) was used to observe the morphologies of catalyst films and CNTs synthesized. X-ray photoelectron spectroscopy (XPS) analysis was used to determine the elemental compositions of Fe films.

3. Results and discussion

Typical SEM images of 5 nm of Fe films after annealing in NH_3 for 4–14 min at 750 °C are shown in Fig. 1, respectively. It is clear that the size and density distribution of Fe nanoparticles change greatly with heating time. Nanoscaled Fe particles have been obtained after thermal treatment in NH_3 for 4 min. However, these particles are not uniformly distributed on substrates: their sizes range from about tens of nanometers to hundreds of nanometers, and the density is low. With increasing heating time to 6 min, Fe particles have been refined, the corresponding density clearly increases, and the uniformity is enhanced. In the case of annealing Fe films for 8 min, the particles obtained are further refined. For 10 min of thermal treatment in NH_3, it is found that small Fe particles with uniform size are obtained and well dispersed on silicon substrates. However, with further increasing heating time to 12 min, large particles are formed again and the uniformity decreases. More and more large particles are observed as heating time continuously increases (Fig. 1f). Finally, most of Fe particles are present in the form of large particles.

In order to precisely investigate the effects of annealing time on the restructuring of Fe films, we statistically analyzed the size distribution of the Fe particles obtained after thermal treatment in

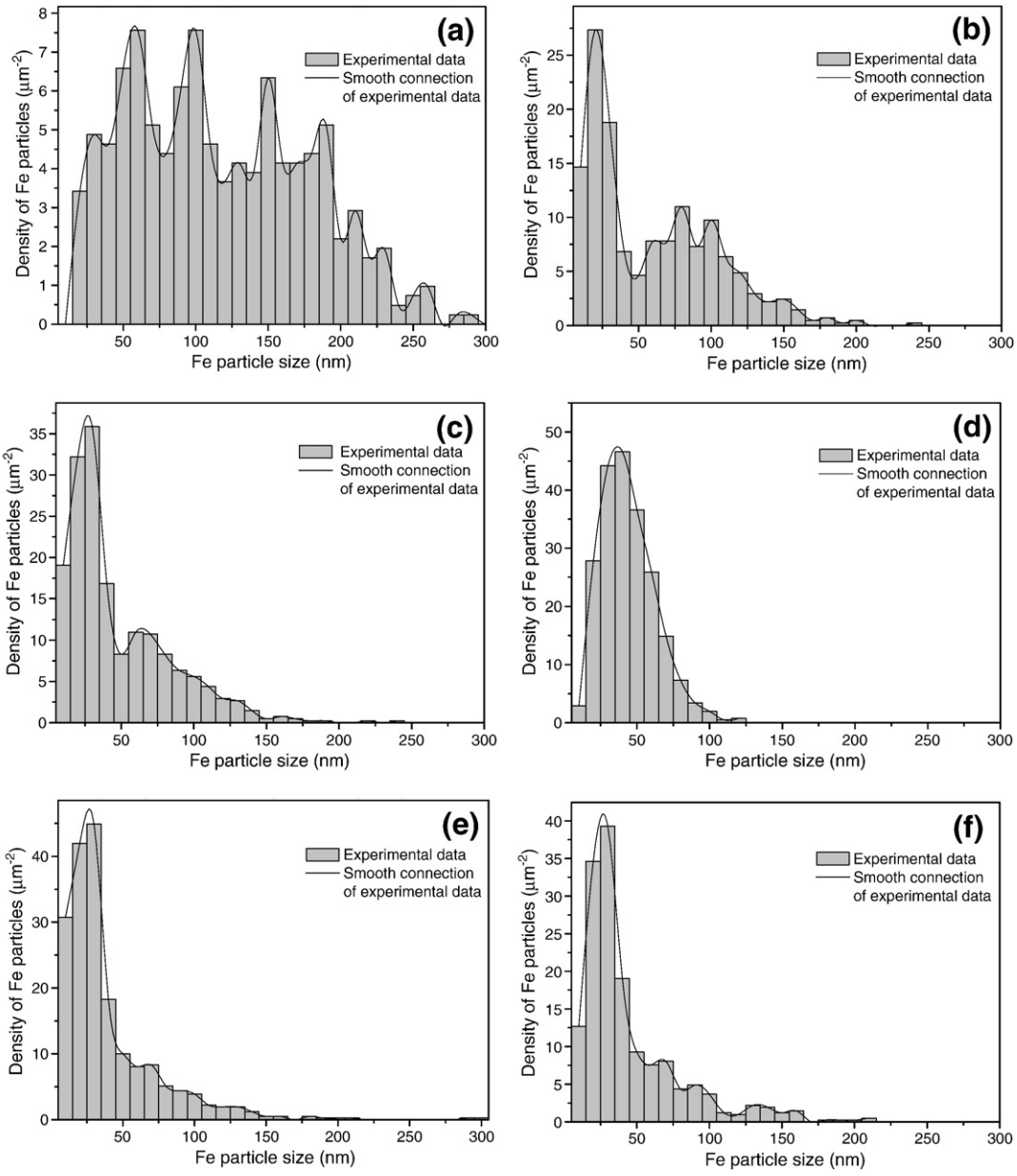

Fig. 2. The distribution histogram of the particles resulted from 5 nm of Fe films after thermal treatment for different time. (a) 4 min; (b) 6 min; (c) 8 min; (d) 10 min; (e) 12 min; (f) 14 min.

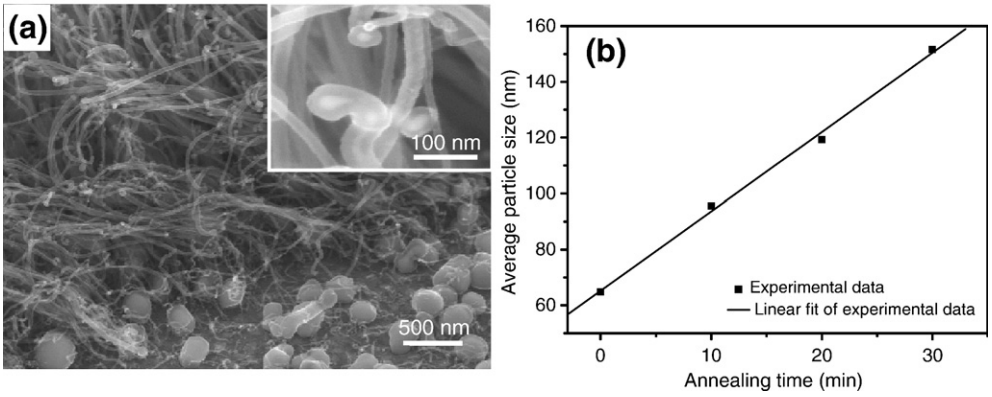

Fig. 3. (a) A SEM image of CNTs grown with the Fe catalyst containing many particles larger than 90 nm. (b) The relationship between the average Fe particle size and annealing time in H_2 at 750 °C. The inset in (a) is the tips of the corresponding CNTs.

NH_3 for different time. Results are shown in Fig. 2. It can be seen that the particle sizes, ranging from about 10 nm to 300 nm, have multi distribution peaks after thermal treatment in NH_3 for 4 min. With increasing heating time from 4 min to 10 min, both the distribution peaks and range of the particle sizes gradually decrease. For 10 min of heating time, Fe catalyst particles have only one distribution peak at about 40 nm with the size range from several nm to 120 nm, similar with Gauss distribution. With heating time increased to 12 min, the distribution range of particle sizes increases again although the particles still have only one distribution peak. From Fig. 2f, it is clear that multi distribution peaks of Fe particles can be observed with further prolonging heating time to 14 min. Both the SEM images and statistical results of Fe particles well demonstrate that Fe particles are refined and the uniformity increases with increasing annealing time from 4 min to 10 min in NH_3. However, with continuously increasing heating time, large particles turned up and the uniformity decreases again.

It is well known that there is a critical particle size for the growth of CNTs in TCVD process [30]. Fig. 3a shows that the Fe particles which are larger than 90 nm were deactivated, and covered by pyrolytic carbon during the nanotube growth. Therefore, 90 nm should be the critical size in our experiment. Here, the particles that are larger than the critical size are defined as large-size particles and those less than the critical size are termed as effective particles. In order to precisely investigate the effects of heating time on the performance of Fe catalyst films in the synthesis of carbon nanotubes, it is necessary to compare the average density and diameter of large-size catalyst particles and effective catalyst particles after annealing treatment for various time (as shown in Tables 1 and 2). From Table 1, it is seen that both the average density and diameter of large-size particles decrease with time. For 10 min of annealing time, the average density and diameter of large-size particles decrease to the minimum, respectively. However, with continuously prolonging heating time, large-size particles increase again due to the sintering of catalyst particles at high growth temperature.

Table 2 shows the statistical results of effective Fe particles formed after thermal treatment for different time. As you see, the change trend of the average diameters of effective particles is complicated. They fluctuate with heating time. However, the average density of effective particles is still contrary to that of large-size particles. It firstly increases and then decreases with heating time. For 10 min of heating time, the average density of effective catalyst particles reaches the maximum (209.63 μm^{-2}). These results sufficiently indicate that large-size particles and effective particles transfer into each other with annealing time. When 5 nm of Fe films are heated in NH_3 for 10 min, most of large-size particles are refined into effective particles, and the density of effective particles accounts for about 99%. Fe nanoparticles with narrow size distribution are most uniformly distributed on substrate surfaces.

To understand the role of NH_3 in the distribution of Fe particles with heating time, we also annealed 5 nm of Fe film in H_2 at 750 °C for different time. Fig. 4c and d show that the density of small particles clearly decreases with increasing annealing time from 0 to 10 min. In contrast, large particle density increase, and even neck-like particles can be observed after annealing for 10 min. Further experimental results show that the average particle size is proportional to annealing time in

Table 1
Statistical analysis of large-size Fe particles formed after thermal treatment for different time

Heating time (min)	Average density (μm^{-2})	Average diameter (nm)
4	59.79	154.47
6	32.21	118.21
8	19.30	115.87
10	3.17	100.88
12	13.91	125.57
14	13.91	127.06

Table 2
Statistical analysis of effective Fe particles formed after thermal treatment for different time

Heating time (min)	Average density (μm^{-2})	Average diameter (nm)
4	42.71	51.79
6	106.16	36.04
8	145.32	36.95
10	209.63	38.39
12	171.8	29.24
14	139.83	31.15

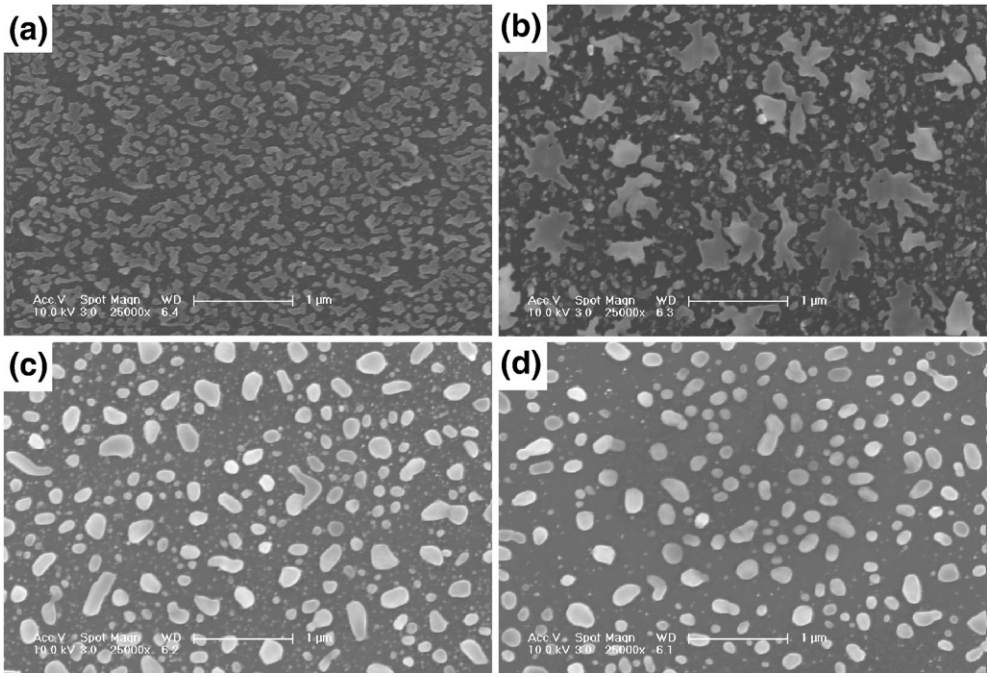

Fig. 4. FESEM images of Fe films after the temperature was stabilized at 600 °C in H_2 (a); after annealing treatment for 60 min at 600 °C in H_2 (b); after the temperature was stabilized at 750 °C in H_2 (c) and after annealing treatment at 750 °C in H_2 for 10 min (d).

H_2 (Fig. 3b), which is clearly different from the results in the case of NH_3. These results sufficiently reflect that H_2 gas cannot inhibit the agglomeration of Fe particles.

If thin metal films are heated, the mobility of their atoms increases and films coarsen and islands coalesce, driven by the lowering of the surface free energy of metal and/or the free energy of the substrates/metal interface [20–22]. However, the gases adsorbed on the metal surface could radically alter the balance of surface free energy and influence the mobility of metal atoms, which depends on the bonds between gas-metal [31]. In general, gases that bond relatively weakly such as H_2 are less effective in this than strongly bounds species such as N [31]. Therefore, H_2 cannot suppress the agglomeration of Fe particles due to the weak H–Fe bonds, and Fe particle average size

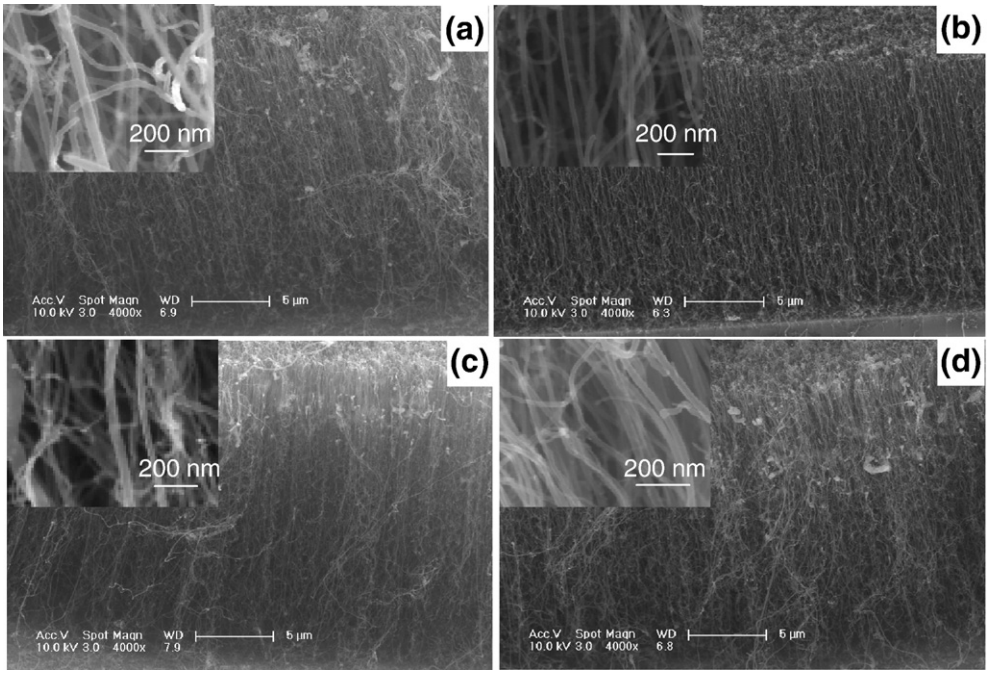

Fig. 5. FESEM images of carbon nanotube arrays grown from Fe films after thermal treatment in NH_3 for different time. (a) 8 min; (b) 10 min; (c) 12 min; (d)14 min.

increases rapidly with annealing time in H_2 at high temperature. In contrast, the effects of NH_3 on the distribution of Fe particles with annealing time are much more complicated, because not only dissociation of NH_3 into NH_x radical and hydrogen molecules on Fe particle surface but also direct nitridation of nanoscale Fe particles with NH_3 would occur [32].

According to the redistribution of Fe particles in NH_3 with annealing time at high temperature, together with the morphologies change of Fe films during temperature rise in H_2 (as shown in Fig. 4), we proposed the effect mechanism of NH_3 on the restructuring of Fe catalyst films with annealing time by analyzing the interaction between Fe particles and NH_3. During temperature rise, Fe films break up and shrink (as shown in Fig. 4a and b), and gradually form nanoscaled particles in H_2 (Fig. 4c) [33]. With the introduction of NH_3 after the temperature was stabilized at 750 °C, NH_3 absorbed on Fe particles and started to decompose into NH_x radical and H_2 molecules. However, at the early stage of introducing NH_3 (less than 4 min), N content on Fe particle was too low to be detected by the X-ray photoelectron spectroscopy (XPS). The low N coverage cannot influence the coalescence of Fe particles effectively, and Fe average particle size still increases rapidly with annealing time (Figs. 4c and 1a), which is similar with that in the case of H_2. With prolonging the time of introducing NH_3, the coverage of NH_x radical on Fe particles was increased clearly, as evidenced by the results of XPS analysis: N element can be easily detected with increasing annealing time to 8 min [25]. Nitrogen bonds so strongly to Fe particles that the higher coverage of NH_x on the particle surface could greatly decrease the surface free energies of Fe particles and radically alters the balance of free energies [31,34]. In order to obtain new balance of free energy, Fe particles could be refined into smaller particles [31]. Therefore, with increasing annealing time from 4 min to 10 min, large-size particles gradually disappeared and the density of small particles increased. Finally, small Fe nanoparticles with narrow size distribution were formed after introducing NH_3 for 10 min. However, as Fe particle size was decreased, the higher specific surface of smaller particles could enhance NH_3 dissociation and lower nitrogen content on their surfaces [35]. Low nitrogen content could not suppress the agglomeration of small Fe particles due to their instabilities at high temperature [36–38]. Therefore, large particles can be observed again after annealing treatment in NH_3 for 12 min (Fig. 1e). With further increasing heating time, more large particles were formed (Fig. 1f). At the same time, the increasing of Fe particle size could enhance the nitridation of Fe particles [35]. From Fig. 1e and f, square surfaces on Fe particles can be clearly seen, indicating that the stable ε-$Fe_{2-4}N$ phase on Fe particles might be formed [35]. It was found that Fe particles were no more refined with continuously prolonging annealing time possibly because of the presence of the stable ε-$Fe_{2-4}N$ phase.

The Fe films obtained after annealing under different conditions have been used to synthesize CNT arrays during the same CVD procedure. Results show that it is difficult for the Fe films after thermal treatment in NH_3 for short time (less than 8 min) and after annealing in H_2 to catalytically grow CNTs. Although CNT arrays have been synthesized after annealing Fe films in NH_3 for 8 min, carbon particles and curved carbon nanotubes can be clearly observed (Fig. 5a). With annealing time increased to 10 min in NH_3, CNTs results are better aligned with uniform diameters, and few carbon particles can be seen (Fig. 5b). However, carbon particles can be observed again when heating time was increased to 12 min (Fig. 5c). As heating time further increased to 14 min, the alignment of nanotubes becomes worse, and even short worm-like carbon fibers can be seen (Fig. 5d). All these results are well consistent with the size distribution of Fe particles formed under different thermal treatment conditions. The presence of N element in Fe particles after thermal treatment in NH_3 could also contribute to CNT growth [39].

4. Conclusions

In summary, Fe films undergo considerable surface morphology restructuring prior to CNT growth. This process is critically dependent on ambient gases and annealing time. We found that NH_3 environments can effectively refine Fe particles or suppress the agglomeration of Fe particles. Furthermore, we successfully obtained Fe particles with narrow size distribution by introducing NH_3 during thermal treatment and controlling annealing time, and synthesized well-aligned CNTs with uniform diameter distribution.

Acknowledgment

This work is supported by the National Natural Science Foundation of China (NSFC, grant no. 10575011).

References

[1] S. Iijima, Nature 354 (1991) 56.
[2] H. Dai, Surf. Sci. 500 (2002) 218.
[3] E.T. Thostenson, Z.F. Ren, T.W. Chou, Compos. Sci. Technol. 61 (2001) 1899.
[4] M. Terrones, Annu. Rev. Mater. Res. 33 (2003) 419.
[5] P. Avouris, J. Appenzeller, R. Martel, S.J. Wind, Proc. IEEE 91 (2003) 1772.
[6] Philippe Serp, Massimiliano Corrias, Philippe Kalck, Appl. Catal. A: General 253 (2003) 337.
[7] J.H. Choi, T.Y. Lee, S.H. Choi, J.H. Han, J.B. Yoo, C.Y. Park, T. Jung, S.G. Yu, W. Yi, I.T. Han, J.M. Kim, Thin Solid Film 435 (2003) 318.
[8] S.A. Moshkalyov, A.L.D. Moreau, H.R. Guttiérrez, M.A. Cotta, J.W. Swart, Mater. Sci. Eng. B 112 (2004) 147.
[9] Z.F. Ren, Z.P. Huang, J.W. Xu, J.H. Wang, P. Bush, M.P. Siegal, P.N. Provencio, Science 282 (1998) 1105.
[10] X.Y. Zhang, L.D. Zhang, G.H. Li, L.X. Zhao, Sci. Eng. A 308 (2001) 9.
[11] S.H. Kim, M.R. Zachariah, Mater. Lett. 61 (2007) 2079.
[12] G.H. Jeong, S. Suzuki, Y. Kobayashi, A. Yamazaki, H. Yoshimura, Y. Homma, Appl. Phys. Lett. 90 (2007) 043108.
[13] K. Bartsch, B. Arnold, R. Kaltofen, C. Täschner, J. Thomas, A. Leonhardt, Carbon 45 (2007) 543.
[14] A. Javey, H. Dai, J. Am. Chem. Soc. 127 (2005) 11942.
[15] A.V. Melechko, V.I. Merkulov, T.E. McKnight, M.A. Guillorn, K.L. Klein, D.H. Lowndes, M.L. Simpson, J. Appl. Phys. 97 (2005) 041301.
[16] R.G. Lacerda, K.B.K. Teo, A.S. Teh, M.H. Yang, S.H. Dalal, D.A. Jefferson, J.H. Durrell, N.L. Rupesinghe, D. Roy, G.A.J. Amaratunga, W.I. Milne, F. Wyczisk, P. Legagneux, M. Chhowalla, J. Appl. Phys. 96 (2004) 4456.
[17] Jason H. Hafner, Michael J. Bronikowski, Bobak R. Azamian, Pavel Nikolaev, Andrew G. Rinzler, Daniel T. Colbert, Ken A. Smith, Richard E. Smalley, Chem. Phys. Lett. 296 (1998) 195.
[18] C. Li Cheung, A. Kurtz, H. Park, C.M. Lieber, J. Phys. Chem. B106 (2002) 2429.

[19] E. Jiran, C.V. Thompson, Thin Solid Films 208 (1992) 23.
[20] J.M. Wen, J.W. Evans, M.C. Bartelt, J.W. Burnett, P.A. Thiel, Phys. Rev. Lett. 76 (1996) 652.
[21] M. Liehr, H. Lefakis, F.K. Legoues, G.W. Rubloff, Phys. Rev. B 33 (1986) 5517.
[22] P.R. Gadkari, A.P. Warren, R.M. Todi, R.V. Petrova, K.R. Coffey, J. Vac. Sci. Technol. A 23 (2005) 1152.
[23] O.A. Nerushev, S. Dittmar, R.-E. Morjan, F. Rohmund, E.E.B. Campbell, J. Appl. Phys. 93 (2003) 4185.
[24] T. de los arcos, M.G. Garnier, J.W. Seo, P. Oelhafen, V. Thommen, D. Mathys, J. Phys. Chem. B 108 (2004) 7728.
[25] H.P. Liu, G.A. Cheng, Y. Zhao, R.T. Zheng, C.L. Liang, F. Zhao, T.H. Zhang, Surf. Coat. Technol. 201 (2006) 938.
[26] Y.T. Jang, J.H. Ahn, Y.H. Lee, B.K. Ju, Chem. Phys. Lett. 372 (2003) 745.
[27] S. Hofmann, M. Cantoro, B. Kleinsorge, C. Casiraghi, A. Parvez, J. Robertson, C. Ducati, J. Appl. Phys. 98 (2005) 034308.
[28] M. Cantoro, S. Hofmann, S. Pisana, C. Ducati, A. Parvez, A.C. Ferrari, J. Robertson, Diam. Relat. Mater. 15 (2006) 1029.
[29] S. Pisana, M. Cantoro, A. Parvez, S. Hofmann, A.C. Ferrari, J. Robertson, Physica E 37 (2007) 1.
[30] Y.Y. Wei, G. Eres, V.I. Merkulov, D.H. Lowndes, Appl. Phys. Lett. 78 (2001) 1394.
[31] W.F. Egelhoff Jr., D.A. Steigerwald, J. Vac. Sci. Technol. A7 (1989) 2167.
[32] L. Darken, R. Gurry, Physical Chemistry of Metals, McGraw-Hill, New York, 1953, p. 374.
[33] V.I. Merkulov, D.H. Lowndes, Y.Y. Wei, G. Eres, E. Voelkl, Appl. Phys. Lett. 76 (2000) 3555.
[34] P.L. Hansen, J.B. Wagner, S. Helveg, J.R. Rostrup-Nielsen, B.S. Clausen, H. Topsoe, Science 295 (2002) 2053.
[35] K. Nishimaki, S. Ohmae, T.A. Yamamoto, M. Katsura, Nanostruct. Mater. 12 (1999) 527.
[36] A.L. Thomann, J.P. Salvetat, Y. Breton, C. Andreazza-Vignolle, P. Brault, Thin Solid Films 428 (2003) 242.
[37] C.E.J. Mitchell, A. Howard, M. Carney, R.G. Egdell, Surf. Sci. 490 (2001) 196.
[38] D.L. Peng, T.J. Konno, K. Wakoh, T. Hihara, K. Sumiyama, Eur. Phys. J., D 16 (2001) 329.
[39] M. Jung, K.Y. Eun, Y.J. Baik, K.R. Lee, J.K. Shin, S.T. Kim, Thin Solid Films 398–399 (2001) 150.